https://doi.org/10.5194/egusphere-2025-5436
Preprint. Discussion started: 18 November 2025

South Atlantic lipid biomarkers support synchronous Plio-Pleistocene global cooling: Revising the ODP Site 1090 sea surface temperature record

Brianna Hoegler[1], Timothy D. Herbert[1], Jamie Pahigian[1]

[1]Department of Earth, Environmental, and Planetary Sciences, Brown University, Providence RI, 02912, USA

Correspondence to: Brianna Hoegler (brianna_hoegler@brown.edu)

Abstract. The Pliocene epoch, 5.33-2.58 Ma, is considered a key analogue for near-future climate scenarios, as it had atmospheric CO_2 levels (>400 ppm) comparable to today and similar continental positioning. Understanding Pliocene climate evolution is also critical to establishing the conditions that enabled large ice sheets to form in the Arctic region during the intensification of Northern Hemisphere glaciation (iNHG) around 2.7 Ma. The causes of iNHG remain unclear, with hypotheses ranging from tectonic changes to CO_2 reductions. Based on anomalous, pre-iNGH cooling signals recorded in a sea surface temperature (SST) record from Ocean Drilling Program (ODP) Site 1090, located in the southeastern Atlantic Ocean, studies have posited that early cooling of the already-glaciated Southern Hemisphere could have driven Earth's climatic descent into the Pleistocene. Here, we provide an orbitally resolved alkenone-based SST record of ODP Site 1090 spanning the time interval ~4.3-2.6 Ma with improved laboratory protocols that significantly revises conclusions based on prior work. Our revised record of SSTs from ODP 1090 shows similar cooling trends to those found of equatorial and high latitude Northern Hemisphere sites, suggesting that a global forcing, such as a reduction in atmospheric CO_2, prompted iNHG, as opposed to an early cooling of the Southern Hemisphere.

1 Introduction

1.1 Pliocene Climate and the Intensification of Northern Hemisphere Glaciation

The Pliocene epoch (5.33-2.58 million years ago, Ma) is an interval with particular relevance to understanding Earth's modern climate, as it is the most recent time in Earth's history that the atmospheric carbon dioxide (CO_2) concentration has been comparable to today's (>400 parts per million, ppm) (NOAA Global Monitoring Laboratory, 2025). Because of the Pliocene's elevated CO_2 levels and its similar continental configuration to today's Earth, this epoch, and especially the Mid-Pliocene Warm Period (mPWP, ~3.3-3.0 Ma), is often considered to be a paleo-analog for near-future climate conditions under moderate warming scenarios (Burke et al., 2018). During this time, mean annual surface temperatures were 2-4 °C warmer, sea levels were elevated, and ice sheet extent was reduced compared to preindustrial conditions, particularly in the northern hemisphere (Haywood et al., 2013).

https://doi.org/10.5194/egusphere-2025-5436
Preprint. Discussion started: 18 November 2025

Better constraining Pliocene climate is additionally important to strengthening our understanding of the conditions that allowed large, continental-scale ice sheets grow in the Arctic region at the very end of the Pliocene. Over the past ~50 My since the early Eocene Climatic Optimum, Earth has experienced a long-term cooling trend and transitioned from a warm greenhouse climate state to an icehouse, in which the high latitudes are covered by large ice sheets. Although Antarctica experienced continental-scale glaciation since the early Oligocene (ca. 34 Ma) (Lear et al., 2008; Zachos et al., 2001), large ice sheets did not start to grow in the northern high latitudes until the intensification of Northern Hemisphere glaciation (iNHG) ca. 2.7 Ma, as evidenced by the appearance of ice-rafted debris (IRD) in North Atlantic marine sediments (Blake-Mizen et al., 2019; Flesche Kleiven et al., 2002; Jansen et al., 2000; Thiede et al., 2011).

Attempts to identify the primary driver(s) of the intensification of Northern Hemisphere glaciation have generated several plausible hypotheses. Some researchers have postulated that tectonic processes, like the closure of the Panama Seaway, could have led to glaciation by intensifying the Gulf Stream, increasing moisture transport to the high latitude north, and strengthening the formation of North Atlantic Deep Water (NADW) (Haug & Tiedemann, 1998; Lunt, Valdes, et al., 2008). However, tectonic processes were likely too slow to cause iNHG, and models have found that the closure of the seaway likely was not a major forcing mechanism for late Pliocene glaciation; instead, models suggest that a decrease in atmospheric CO_2 concentrations to 280 ppm was needed to drive glaciation on Greenland (Lunt, Foster, et al., 2008; Lunt, Valdes, et al., 2008; Tan et al., 2017).

This hypothesis— that a reduction in greenhouse forcing lowered global temperatures and drove the iNHG— is supported by a growing body of literature. Paleoclimatic proxy data suggests that atmospheric CO_2 decline coincided with late Pliocene glaciation (Rae et al., 2021) and that global cooling was occurring in all ocean areas other than the Indo-Pacific warm pool (IPWP) around 4 Ma and continuing through the iNHG (Clark et al., 2024). This global cooling signal is consistent with climate models, which have shown that reducing CO_2 levels in the atmosphere would result in cooling across both the northern and southern hemispheres (Broccoli & Manabe, 1987; Stap et al., 2018).

One other prominent hypothesis exists to explain the primary driver of iNHG: that regional climate change in the Southern Hemisphere ultimately drove ice sheet growth in the north. In this scenario, growth of the Antarctic ice sheet would fuel the positive ice-albedo feedback effect, leading to regional cooling concentrated around the high-latitude Southern Hemisphere (McKay et al., 2012). Past a certain threshold, ice sheet expansion could have altered global ocean and atmospheric circulation, culminating in global temperature reductions large enough to lead to Northern Hemisphere glaciation (Woodard et al., 2014).

The alkenone-based reconstruction of ODP Site 1090's SST of Martínez-Garcia et al. (2010) is a critical piece of evidence informing this hypothesis. This record features cooling over parts of the late Pliocene that outpace much of the rest of the

https://doi.org/10.5194/egusphere-2025-5436
Preprint. Discussion started: 18 November 2025

world, a possible indication of high-latitude Southern Hemisphere climate cooling leading up to iNGH, and it has been utilized in several studies positing that regional forcing could have played a significant role in driving iNHG (McClymont et al., 2023; Woodard et al., 2014; Burton et al., 2024).

We were motivated to re-examine the alkenone-based SST record by two aspects of the Martínez-Garcia data set that appear anomalous. The first of these is the offset between this record and an alkenone-based record produced by Etourneau et al. (2010), also at Site 1090, during the 800 ky leading up to iNGH, with the Etourneau record indicating SSTs up to 5 C° warmer than Martínez-Garcia (Fig. 2). The second aspect is the unusually high $C_{37:4}$ content reported by Martínez-Garcia and coauthors, which would be unusual given the moderate temperatures reconstructed for the site in the Pliocene.

1.2 ODP Site 1090 and the Paleo-Temperature Record of the Southern Atlantic Ocean

The location of Ocean Drilling Program (ODP) Site 1090 (42°54.5'S, 8°54.0'E, Fig. 1) is optimal for studying a variety of oceanographic and climatic phenomena through time, including Antarctic ice-sheet development, Antarctic Circumpolar Current (ACC) frontal boundary movements, and changes in the contribution of NADW to the Southern Ocean (Shipboard Scientific Party, 1999). Located on the southern flank of the Agulhas Ridge at a water depth of 3702 m, above the carbonate compensation depth and close to the boundary between the Circumpolar Deep Water (CDW) and North Atlantic Deep Water (NADW) masses, ODP Site 1090 contains one of the most southerly records recovered of late Pliocene/early Pleistocene climate. Today, the site sits within the sub-Antarctic Zone of the AAC, between the Subantarctic Front (SAF) and Subtropical Front (STF), and below the southernmost Polar Front (PF). The overlaying CDW is the principal water mass making up the AAC, while the nearby NADW tongue helps feed it at intermediate depths (Reid, 1989). Site 1090's sea surface temperature (SST) has been strongly influenced by meridional shifts in the AAC, driven by the northward expansion of the PF, SAF, and STF. Biomarker, isotope, and microfossil data suggests these fronts may have migrated upwards of 7° latitude during cold stadials in the Pleistocene, resulting in SST changes of up to 8°C between glacial/interglacial periods (Bard & Rickaby, 2009; Becquey & Gersonde, 2002).

https://doi.org/10.5194/egusphere-2025-5436
Preprint. Discussion started: 18 November 2025

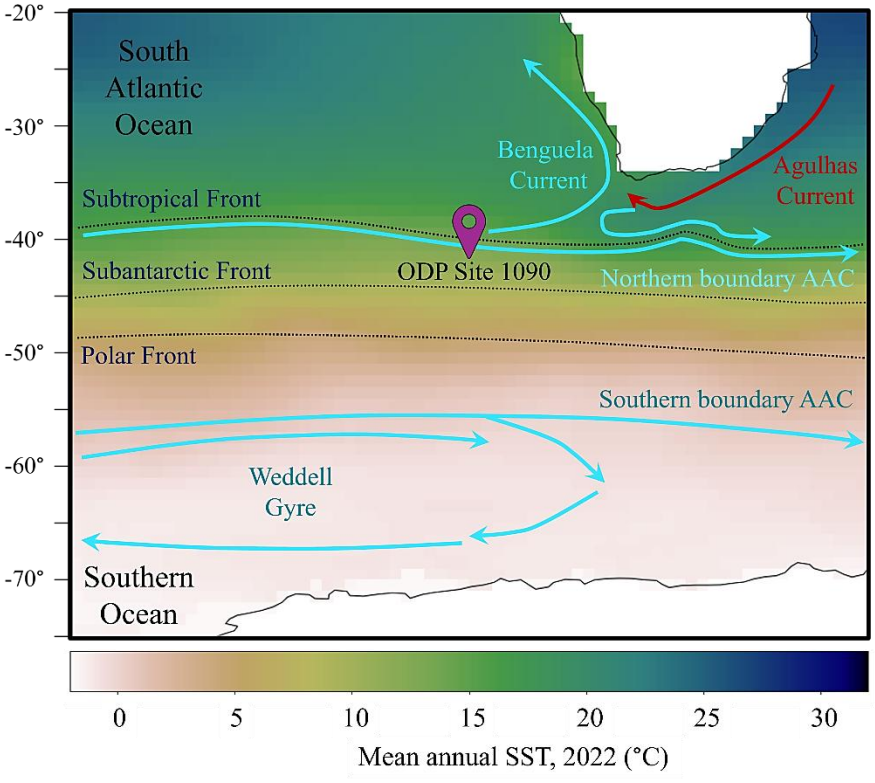

Figure 1: Map of the eastern South Atlantic Ocean and Southern Ocean, centred on ODP Site 1090. Solid lines depict the major ocean currents in the study area. Blue and red lines represent cold and warm currents, respectively. The three dashed lines show the approximate position of the three fronts of the Antarctic Circumpolar Current. Modern SST data was provided by NOAA PSL.

Five holes were drilled at ODP Site 1090. The composite of the cores drilled from these holes produces a continuous stratigraphic section, spanning approximately 4 Ma. We revised the shipboard splice between 1090D core 7 to 1090E core 7 (approx. 2.69─4.27 Ma) based on the magnetic susceptibility profiles and documented the new splice with overlapping alkenone SST estimates (Tables S2, S3; Figs. S3, S4). The upper portion of the core, above approximately 68.5 meters composite depth (mcd), ranges from the Holocene to late Pliocene in age. Below this, erosion and/or nondeposition of sediments led to a hiatus spanning much of the early Pliocene through mid-Miocene; deeper sediments span the early Miocene through the middle Eocene (Shipboard Scientific Party, 1999; Billups et al., 2004).

2 Depth Composite and Age Model

To produce the most robust stratigraphy possible, we improved upon the existing shipboard composite depth estimations (Shipboard Scientific Party, 1999). Using our SST to enhance the shipboard magnetic susceptibility and cryomagnetic inclination data, we were able to establish a more accurate composite of ODP Site 1090 Holes D and E by correlating the two

https://doi.org/10.5194/egusphere-2025-5436
Preprint. Discussion started: 18 November 2025

holes' properties (Fig. S3, Table S2). Our revised composite section spans from around 55 to 71 MCD. Using this revised composite, we spliced together our Hole D and Hole E GC-FID SST records to produce one continuous record (see data availability statement for information regarding data access). An abrupt change in magnetic susceptibility data locates the Miocene/early Pliocene hiatus at ~70 MCD, consistent with shipboard biostratigraphy.

We used biostratigraphic and magnetostratigraphic data to establish initial age constraints for our age model (Shipboard Scientific Party, 1999). We found the magnetostratigraphic data to provide reliable age-depth ties from 3.04 to 3.594 Ma; however, we found it to be an unreliable indicator deeper in the core (MCD > 67, as measurements neared the hiatus), as putative polarity shifts could not be correlated between offset holes in the magnetic susceptibility framework. To more precisely assign ages to the Site 1090 SST data, we tuned the 1090 SST data as a function of composite depth to Lisiecki and Raymo's (2005) "LR04" $\delta^{18}O_{benthic}$ record (Fig S4, Table S3), which allowed for finer age assignments than the biostratigraphic and magnetostratigraphic data alone while remaining consistent with the age estimates yielded from those data. Our age-depth model suggests that our SST record spans approximately 2.6–4.3 Ma.

3 Materials and Methods

3.1 Biomarker Extraction

Alkenone paleothermometry is a well-calibrated and reliable paleo-proxy for open-ocean SST (Herbert, 2003; Müller et al., 1998). Alkenones— lipid biomarkers produced by certain species in haptophyte class *Prymnesiophyceae*— are 37-, 38-, and 39-carbon chained (C_{37}, C_{38}, C_{39}) ketones (Marlowe et al., 1984). The relative unsaturation of the C_{37} ketone, represented by the $U^{k'}_{37}$ and U^{k}_{37} indices (Table S1), linearly decreases with increasing temperature in all but the warmest (>24°C) ocean waters (Müller et al., 1998; Tierney & Tingley, 2018). Because of this relationship, the global distribution of alkenones, and alkenones' tendency for incredibly high preservation, they are one of the most highly utilized proxy biomarkers for near-surface temperatures in the past open ocean (Prahl et al., 1988; Sikes et al., 1991). In this study, we utilize the global core-top based calibration of Müller et al. to derive SST (1998). Because residuals between core-top $U^{k'}_{37}$-SST and satellite mean annual SST are miniscule in the southeast Atlantic, we expect $U^{k'}_{37}$ to act as a proxy of mean annual temperature at ODP 1090 (Tierney & Tingley, 2018).

We sampled the sediment core from ODP Site 1090 approximately every 5 cm, beginning at ~50 meters below the seafloor (MBSF), corresponding to about 55.3 meters composite depth (MCD), and ending at ~61 MBSF (~70 MCD). This sample range and resolution was selected to overlap with and extend the Martínez-Garcia late Pliocene SST record, spanning from the end of the Pliocene ca. 2.58 Ma to the hiatus in the sediment core at an estimated 4.3 Ma which prematurely ends the Pliocene record.

https://doi.org/10.5194/egusphere-2025-5436
Preprint. Discussion started: 18 November 2025

Sediment samples were frozen overnight, and freeze-dried for 24 hours prior to homogenization using a mortar and pestle. Approximately 8-10 grams of sediment were mixed with sand (previously baked to prevent contamination by organic compounds) to improve solvent flow and packed into 34 mL cells with glass fiber filters. Alkenones were extracted from samples using 100% Dichloromethane (DCM) in an Accelerator Solvent Extraction system (Dionex ASE 350). Every round of 24 samples extracted on the ASE included one blank extraction of pre-combusted sand to check that no contamination was introduced during the extraction process.

Although the calibration equation chosen for both studies are nearly identical (Tables 1, S1), they differ in one key aspect: Martínez-Garcia utilized the U^{k}_{37} alkenone unsaturation index (Brassell et al., 1986), which includes the tetra-unsaturated alkenone ($C_{37:4}$):

$$U^{k}_{37} = \frac{[C_{37:2} - C_{37:4}]}{[C_{37:2} + C_{37:3} + C_{37:4}]} \quad (1)$$

However, Etourneau used the $U^{k'}_{37}$ index (Prahl et al., 1988), which excludes $C_{37:4}$:

$$U^{k'}_{37} = \frac{[C_{37:2}]}{[C_{37:2} + C_{37:3}]} \quad (2)$$

Sites where $C_{37:4}$ is present in the largest quantities experience at least seasonal sea ice cover— unlike ODP Site 1090— leading some to suggest this ketone may have utility as a sea ice proxy but perhaps should not be included as a temperature proxy specifically (Liao, Wang, et al., 2023; Wang et al., 2021).

Table 1: Summary of new and published alkenone-derived SST data utilized in this study

n	Depth (MCD)	Sample Resolution	Extraction	Cleanup	Method	Columns	AUI	Calibration
Etourneau et al., 2010								
51	40.21 – 63.08	~40 kyr	ASE	none	MDGC, GC-FID	RTX-1, RTX-200	$U^{K'}_{37}$	Müller et al., 1998
Martínez-Garcia et al., 2010								
1126	0 – 65.69	~3.4 kyr	MSE	none	GC-FID	HP-1	U^{K}_{37}	Prahl & Wakeham, 1987
This study								
408	0.07 – 71.14	2 – 3 kyr	ASE	Silica gel and silver nitrate columns	GC-FID, HPLC	DB-1, RTX-200	$U^{K'}_{37}$	Müller et al., 1998

Note. Abbreviations as follows: n = number of samples, mcd = meters composite depth, AUI = alkenone unsaturation index, ASE = accelerated solvent extractor, MSE = microwave solvent extraction, MDGC = multidimensional gas chromatography, GC-FID = gas chromatograph-flame ionization detector, HPLC = high pressure liquid chromatography

https://doi.org/10.5194/egusphere-2025-5436
Preprint. Discussion started: 18 November 2025

3.2 Sample Purification and Preparation for Analysis

Extracted samples were dried in a TurboVap blowdown evaporator at 35°C under constant flow of N_2. Samples were rehydrated in DCM and glass pipetted into 4 mL vials. After initial GC-FID results yielded chromatograms with noisy baselines, likely due to other organic residues that can co-elute with the ketones we seek to measure, we conducted compound purification via flash column silica gel chromatography followed by silver nitrate column (D'Andrea et al., 2007). After cleanup, samples were again dried at 35°C under a mini evaporator before being spiked by 210 µL of an internal lab standard (hexatriacontane [C_{36} alkane] and heptatriacontane [C_{37} alkane], 2 µg/mL in toluene). 50 µL of each sample extract was transferred to its own 2 mL glass vial with a 100 µL insert. Samples were capped and kept refrigerated until ready for alkenone measurement.

3.3 Alkenone Measurements

There are multiple challenges that must be considered to ensure reliable analyses at ODP Site 1090: low biomarker concentrations and a complex sediment matrix. At sites with very low total C_{37} alkenone concentrations ($C_{37total}$), such as ODP Site 1090, it can prove difficult to differentiate the biomarker signal from baseline noise using the typical GC-FID method. This problem is exacerbated by compounds that co-elute with alkenones that may be present in the sediment extract. Therefore, there is a need to not only attempt to reproduce Martínez-Garcia et al.'s SST record (2010), but also to unambiguously assess whether the $C_{37:4}$ ketone is present in measurable quantities at ODP Site 1090. To ensure the precision and accuracy of our results, we not only measured alkenone concentrations using traditional gas chromatography (GC) techniques but also confirmed our findings using high performance liquid chromatography (HPLC). Sixteen samples were randomly selected to undergo both GC-FID and HPLC analysis.

3.3.1 Gas Chromatography

Samples were analysed using gas chromatography with flame ionization detection (GC-FID). Most samples were transported through a DB-1 column, though some initial analyses were conducted using an RTX-200 column. Due to low alkenone concentrations yielding small chromatographic peak areas (area < 10), we elected to increase the injection volume from our lab's standard 1 µL to 10 µL. The GC-FID program was as follows: the oven was set to an initial temperature of 90°C with a hold time of 2 minutes; the oven increased in temperature at a rate of 40°C/min until it reached 255°C; then, the oven would increase by 1°C/min until a temperature of 300°C was reached; finally, the oven increased in temperature by 10°C/min until 320°C was reached, and the oven held this temperature for 11 minutes. An alkenone-containing lab standard and a previously run sample were run every 7 samples to ensure data quality.

https://doi.org/10.5194/egusphere-2025-5436
Preprint. Discussion started: 18 November 2025

A MATLAB-based Chromatography Graphics User Interface (GUI) was utilized for data integration (Dillon, 2023). After adjusting the baseline, the peaks corresponding to our target ketones were selected by hand on two lab standard chromatograms; then, the GUI automatically picked the peaks in the remaining chromatograms. All chromatograms were then checked visually to ensure the accuracy of peak area assignments.

3.3.2 HPLC-MS

While GC-FID is an analytical workhorse, response on the detector is not compound-specific. In difficult matrices and where the analytes of interest are at low concentrations, this can lead to erroneous compound quantification. To demonstrate the reliability of peak assignments and to determine if the less common $C_{37:4}$ ketone was indeed present in our samples, we optimized a reversed-phase High-performance liquid chromatography -mass spectrometry (HPLC-MS) originally described by Liao et al. (2023). This method provided excellent resolution, selectivity, linearity, and sensitivity for alkenones in complex matrix of Site 1090 samples. Crucially, we were able to unambiguously determine the quantity of the $C_{37:4}$ ketone by calibration of the HPLC response to a purified extract of Greenland lake sample (D'Andrea & Huang, 2005). Samples where the SST estimate derives from HPLC are denoted in both Table S4 and our final SST reconstruction, available on PANGAEA (citation upon issue of DOI).

3.3.3 SST Calibration

To derive temperature from our measured ketones, we utilized the $U^{k'}_{37}$ unsaturation index (Prahl et al., 1988). SSTs were calculated using the Müller et al. (1998) global core top calibration:

$$U^{k'}_{37} = 0.033(SST) + 0.044 \quad (3)$$

Although other calibrations of $U^{k'}_{37}$-SST have been established, we elected to utilize the Müller et al. (1998) equation due to negligible differences between this and other calibrations, both linear and non-linear, in the $U^{k'}_{37}$ range appropriate to Site 1090 data (Conte et al., 2006; Tierney & Tingley, 2018).

3.4 Quality Control Measures

Each collected datum was individually checked for quality control in three ways. The total measured concentration of the C_{37} ketone (C_{37} total) was found for each sample; data from samples with undetectable or especially low C_{37} total (<0.0012, |mean-stdev|) were removed from the final SST record. We calculated the $U^{k'}_{37}$ height to area ratio of the GC peaks, as large (>10%) deviations from the peak area-based index can indicate co-elution of ketones with other compounds, and samples found to have large height deviations from area were also removed. Finally, we compared the $U^{k'}_{37}$ area to the U^{k}_{38ME} (the 38-carbon chain-length methyl-ketone based unsaturation index) area, which follow a linear relationship in modern sediments (Novak et al., 2022) as a final check to identify anomalous analyses. In total, seven samples were completely rejected from the final SST reconstruction, which consists of 408 samples.

https://doi.org/10.5194/egusphere-2025-5436
Preprint. Discussion started: 18 November 2025

3.5 Examination of Potential Bias Caused by Cleanup Methods

Previous work by Martin et al. (2024) has found that silver-nitrate purification may modify the C_{37} alkenone distribution and thus the unsaturation indices, especially the U^k_{37} index, by preferentially retaining alkenones with more double bonds. We conducted additional analyses to determine if and to what extent our column chromatography-based cleanup methods may be biasing our measurements of 37-, 38-, and 39-carbon chained ketones. Approximately 1 mL of our in-house alkenone standard was pipetted into eight 4mL vials and evaporated under a constant N_2 stream on a hot plate set to 35°C. Six vials of this standard were rehydrated in 1 mL of hexane before undergoing the previously described cleanup procedures; the additional two vials were left as a control. This procedure was also repeated using the Greenland standard (D'Andrea & Huang, 2005), which, unlike the in-house standard, contains a large quantity of $C_{37:4}$ methyl-ketones.

Experimental evaluation showed little to no evidence of cleanup biasing our results. The average SST of all experimental samples (N = 13)— our typical lab standard, the de- and re-hydrated standard, and the cleaned standards— were within a few hundredths of a degree of each other, both using our typical DB-1 method and utilizing the 10 µL sample volume required by ODP Site 1090 alkenone measurements (Fig. S1). Our experimental results using the Greenland standard yielded similar results, with negligible change in our derived SSTs following silica gel and silver nitrate cleanup (Fig. S2).

3.6 Calculations and Analysis

3.6.1 Back-calculation of $U^{k'}_{37}$ from U^k_{37} and $\%C_{37:4}$

In their study, Martínez-Garcia et al. (2010) elected to utilize the culture-based temperature-U^k_{37} calibration of Prahl and Wakeham (1987):

$$U^k_{37} = 0.033(SST) + 0.043 \quad (4)$$

To establish a more direct comparison between our data, we estimated the approximate SST Martínez-Garcia et al. (2010) would have reported had they utilized the simplified unsaturation index ($U^{k'}_{37}$). We first inferred their U^k_{37} from their SST data, and then we used their reported $\%C_{37:4}$ to estimate $U^{k'}_{37}$:

$$inferred\ U^{k'}_{37} = \frac{U^k_{37} + (\%C_{37:4} \times 0.01)}{1 - (\%C_{37:4} \times 0.01)} \quad (5)$$

Then, we applied the SST calibration of Müller et al. (1998; Eq. 3) to reconstruct temperature from our estimated values of $U^{k'}_{37}$.

4 Results

https://doi.org/10.5194/egusphere-2025-5436
Preprint. Discussion started: 18 November 2025

Our age-depth model shows similarities to Martínez-Garcia et al.'s 2011 age-depth model for ODP 1090, with model agreement being strongest, with little to no disagreement, around 3.2 My (Fig. 2). Nevertheless, there are differences: our age-depth model produced mean estimated ages that were ~27 ky younger compared to Martínez-Garcia's estimates. Peak age model disagreement occurred around 56.64 MCD, where our age estimates differed by ~120 ky. Depths with the highest age model disagreement tended to feature low alkenone concentrations (Fig. S5). In addition to adjusting the ODP 1090 age-depth assignments, our ~5 m extension of alkenone measurements downcore allowed us to add an additional ~460 ky to the prior SST reconstruction.

In contrast to results reported in Martinez-Garcia et al. (2010), we observed minimal concentrations of the $C_{37:4}$ ketone. While we often observed a small peak in the chromatograms at the elution time when we would expect to see the tetra-unsaturated C_{37} methyl-ketone, this peak was rarely taller than the surrounding baseline noise— too small to yield reliable results, let alone comparable $\%C_{37:4}$ values to the Martínez-Garcia record. Our GC-FID chromatograms yielded results indicating an average of 3.02% of the total C_{37} ketones could correspond to the $C_{37:4}$ ketone in our ODP Site 1090 Pliocene sediments.

Our HPLC measurements (N=16) both confirm our GC-FID results and verify that there is little to no $C_{37:4}$ present in Pliocene ODP Site 1090 sediments. The HPLC results show nearly identical $C_{37:2}$ and $C_{37:3}$ concentrations and ratios compared to our established methodology using GC-FID. The $C_{37:4}$ ketone is present in only small quantities, with $\%C_{37:4}$ ranging from a below detection limits to a maximum of 3.78%; the average was 0.41%. The similar results produced by both the GC-FID and HPLC methods validate the quality of our alkenone measurements and interpretation of paleo-temperatures. We therefore conclude that the high concentrations of the $C_{37:4}$ ketone previously reported were most likely an analytical artifact.

The SST estimates generated from our biomarker measurements are typically warmer than those produced by Martínez-Garcia et al., (2010). On average, our SST estimates were 1.27°C warmer during the Pliocene interval for which we both have data, corresponding to 55.93-65.95 MCD (Fig. 4). To determine if there is a significant difference between our Pliocene SST record and that of Martínez-Garcia et al. (2010), we conducted Welch's t-test, comparing SST estimates of the same depth interval. An alpha of 0.05 was used to determine significance. The resulting p-value was <0.05, indicating a significant difference between the SST records. Critically, the cold intervals in the Martínez-Garcia record between 2.8-3.05 Ma are not observed in our revised record, and our record provides no indication of directional cooling.

To investigate the potential of long-term directional cooling revealed in either our record or the Martínez-Garcia record, we plotted the least-squares linear regression of the data from 2630-3810 kya (Fig. 2). The R^2 of both records is small, likely due to the large degree of orbital variability superimposed on any trend. The P-values of the regression for both records are <0.05. The least-squares linear regression of the data spanning our record from 2600-4267 kya, the ned of our record, is similar: $y = 0.0009x + 11.611$, with an R^2 of 0.0631.

https://doi.org/10.5194/egusphere-2025-5436
Preprint. Discussion started: 18 November 2025

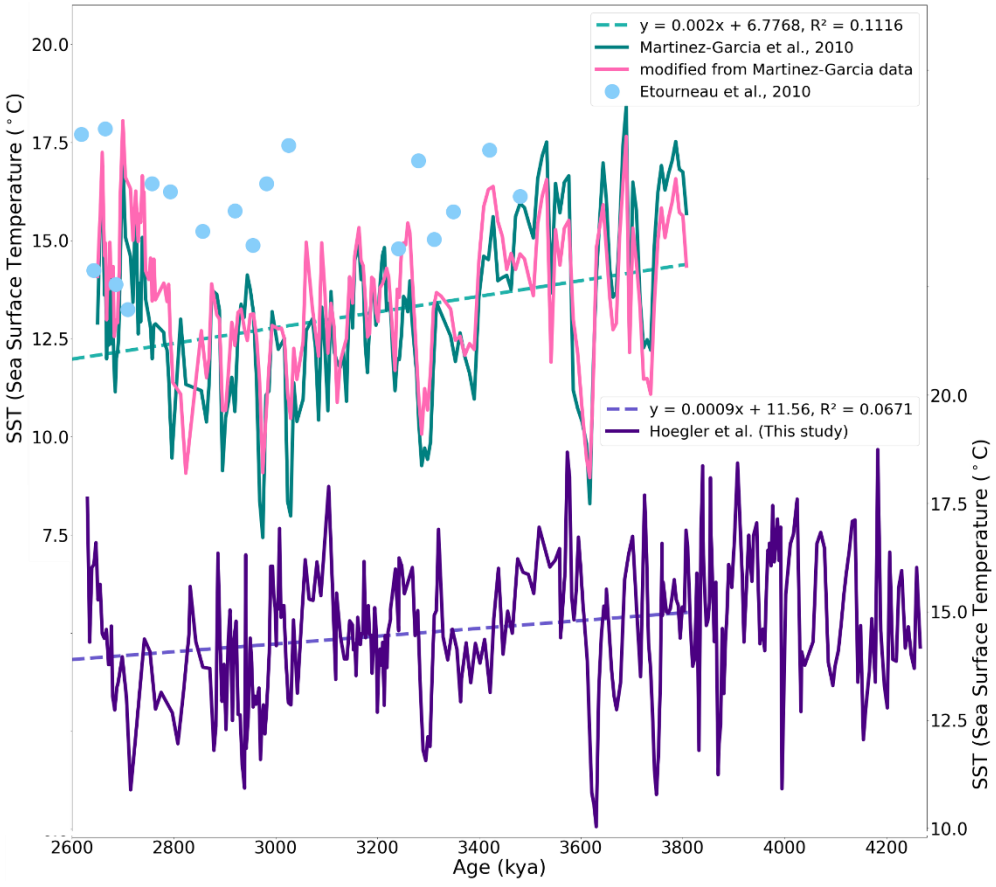

Figure 2: Alkenone-based SST estimates from ODP Site 1090. Data from previous studies (Martínez-Garcia et al., 2010 and Etourneau et al., 2010) are plotted above; the teal line denotes the original U^{k}_{37}-based SST Martínez-Garcia estimates, while the pink line indicates our estimate of $U^{k'}_{37}$-based SST using their data. The SST record constructed during this study is plotted below, in indigo. For both the original Martínez-Garcia record and our new record, we plotted the least-squares linear regression of the data from 2630-3810 kya.

5 Discussion

5.1 A revised, alkenone-based SST record of the late Pliocene subantarctic East Atlantic

Compared to the SST record of Martínez-Garcia et al. (2010), our SST estimates record only a gentle cooling trend leading up to iNGH (Fig. 2), with our record showing cooling at ~45% of the rate of the prior record between 2.63-3.81 Ma. In addition, both our new high-resolution dataset and the lower-resolution SST data of Etourneau et al., (2010) indicate that SSTs were warmer during the late Pliocene at ODP Site 1090 than Martínez-Garcia et al. (2010) estimate. Minimum temperatures in the

https://doi.org/10.5194/egusphere-2025-5436
Preprint. Discussion started: 18 November 2025

interval spanning ca. 2.89-3.03 Ma are often 1-2°C warmer in our record (Fig. S5), and there is little to no indication of anomalously cold events at ODP Site 1090 uniquely preceding iNHG (Figs. 2, 3). We believe that most of the differences between data sets result from the very difficult sample matrix presented by Site 1090 and the optimization of sample purification and strategic use of HPLC in the present study.

315

https://doi.org/10.5194/egusphere-2025-5436
Preprint. Discussion started: 18 November 2025

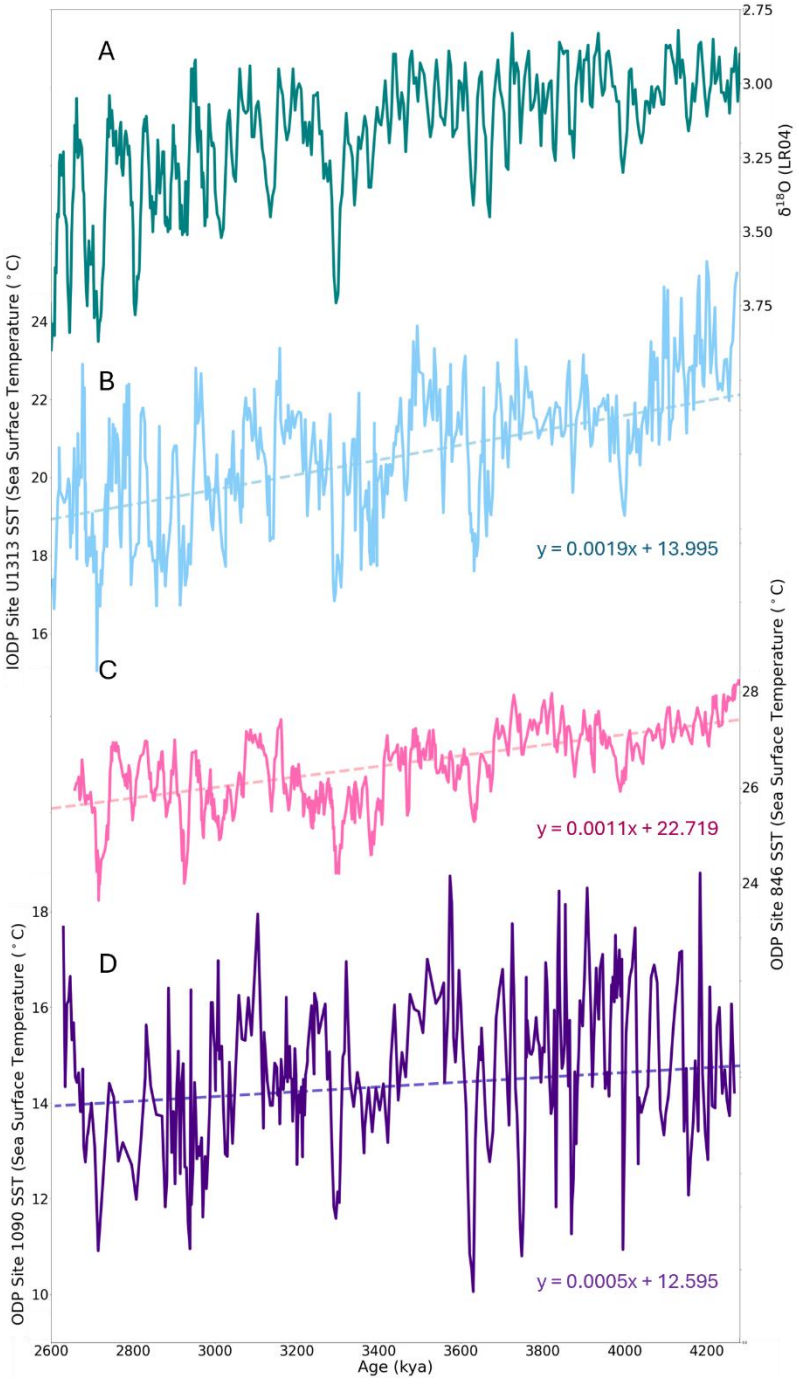

Figure 3: When comparing our Site 1090 record (D) to those from other regions (here, the northeast Atlantic [IODP U1313, panel B] and eastern equatorial Pacific [ODP 846, panel C]) we observe little evidence of early cooling in the high latitude southern hemisphere compared to the rest of the world. Notice the similar, slightly negative cooling trend at all three sites, indicative of cooling occurring synchronously across the globe; in fact, ODP Site 1090 displays a less negative cooling trend throughout the late Pliocene

https://doi.org/10.5194/egusphere-2025-5436
Preprint. Discussion started: 18 November 2025

than at ODP Site 846 (eastern equatorial Pacific) or IODP Site U1313 (north Atlantic). Also displayed is the LR04 benthic oxygen isotope stack (panel A) from 2.6-4.28 Ma.

Both our GC-FID and HPLC results indicate that $C_{37:4}$ was not present in reliably measurable quantities in ODP Site 1090 sediments. As $C_{37:4}$ is present only in low concentrations in most marine sediments, including those of Site 1090, its measurement is subject to disproportionate risk of overestimation due to co-eluting compounds and baseline noise (Brassell et al., 1986). The overutilization of less abundant compounds, such as the tetra-unsaturated alkenone, in proxy calibrations can dampen trends and obscure important relationships, risking the introduction of bias in analyses (Raberg et al., 2021). Therefore, it is advisable to positively identify measurable $C_{37:4}$ in marine sediments before utilizing the U^{k}_{37} index in preference to the $U^{k'}_{37}$ index.

5.2 Implications of revising the record: synchronous cooling across hemispheres leading up to the iNHG

Our record of ODP Site 1090 SSTs in the late Pliocene does not exhibit a cooling trend that is distinct from those at other open ocean sites, including those in the Northern Hemisphere and low latitudes (Fig. 3). In fact, when comparing the Site 1090 SST record with those of ODP Site 846 (eastern equatorial Pacific) and IODP Site U1313 (northern Atlantic), the cooling trend from 2650–4125 kya is the most gradual at ODP Site 1090; while the slopes of the best fit lines of SSTs from ODP 846 and IODP U1313 are 0.0011°C/kya and 0.0019°C/kya, respectively, it is only 0.0005°C/kya at ODP Site 1090.

The SST record of ODP Site 1090 shares orbital-scale features with records from other regions of the global ocean. Spectral analyses using the multitaper method Fourier transform were conducted to identify the dominant periods of variability in the SST records of ODP Site 1090, ODP Site 846, and IODP Site U1313 at the 95% confidence interval (Fig. 4). Our spectral analysis reveals that all three sites had dominant periodicities in the obliquity band (41 kyr cycles). Only ODP 846 showed significant sensitivity to the precession band (23 kyr cycles), and no site showed significant sensitivity to the eccentricity band (100 kyr cycles). Coherence between the SST records of each site and the average eccentricity, obliquity (tilt) and precession (ETP) is strongest in the obliquity band for all sites (Fig. 4). This demonstrates that Earth's changes in obliquity acted as a significant control on temperature globally during the late Pliocene.

The revised SST record of ODP Site 1090 supports the hypothesis that global SST records displayed only a modest long-term cooling trend throughout the late Pliocene. Intriguingly, interglacial SST values of the late Pliocene were almost as high as in the preceding million years (Fig. 3). This contrasts with the suggestion that asynchronous global cooling, caused by a regional temperature forcing like the ice-albedo feedback in the Antarctic, led to the iNHG (e.g., McClymont et al., 2023; McKay et al., 2012; Woodard et al., 2014). Had an orbitally paced, regional forcing caused the expansion of the Antarctic ice sheet and driven global cooling leading to the iNHG, we would expect to see cooling signals unique to the ODP 1090 record compared

https://doi.org/10.5194/egusphere-2025-5436
Preprint. Discussion started: 18 November 2025

to more northerly sites. However, all sites' SST reconstructions reveal similarly paced warm- and cool-intervals (Fig. 3), hinting that a global mechanism drove this variability in temperature.

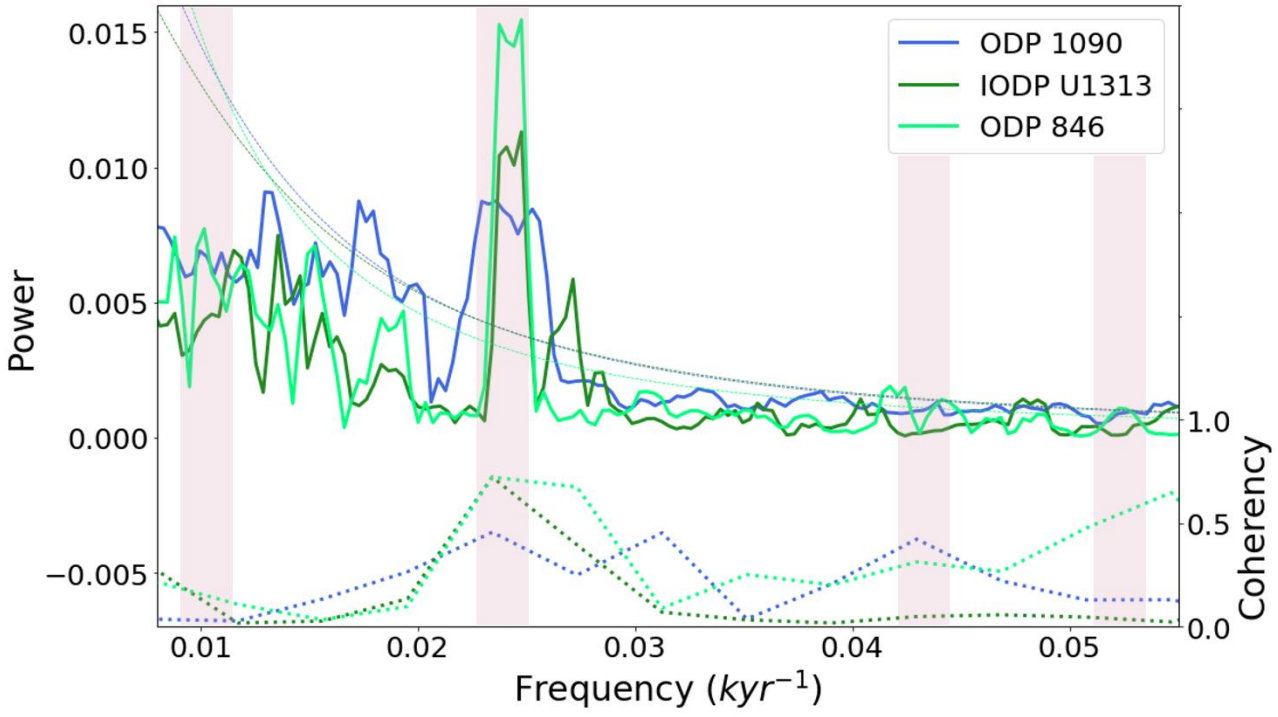

Figure 4: Astronomical power spectra (solid lines, above) and coherence analyses (dotted lines, below) relative to ETP (eccentricity, tilt [obliquity], precession) of ODP Site 1090, IODP Site U1313, and ODP Site 846. SST data from 2.650-4.260 kya were normalized, detrended, and linearly interpolated to an age scale with equal <3 kyr time steps. The thresholds for 95% confidence intervals are plotted over the power spectra as dashed lines. To analyse spectral power, a multitaper method Fourier transform was utilized (Meyers et al., 2021). To calculate coherency, we utilized the gsignal package in R. The pink bars denote the frequency of each ETP component.

Our results are consistent with a significant body of compelling research supporting the hypothesis that synchronous cooling, driven by decreasing atmospheric carbon dioxide concentrations, allowed for Northern Hemisphere ice sheets to grow under favorable orbital configurations. Earth system models have demonstrated that lowered atmospheric CO_2 would have led to synchronous global cooling (Lunt, Foster, et al., 2008; Willeit et al., 2015). Similarly, a recent synthesis of global paleo-temperature records showed that changes in long-term cooling and variability during the past 4.5 million years is likely paced by geologically driven changes in Earth's carbon cycle (Clark et al., 2024). DeConto et al., (2008) utilized isotope-capable global climate/ice-sheet models to show that the atmospheric CO_2 threshold below which glaciation occurs is higher (~750 ppm) in the Southern Hemisphere compared to the high latitude north (~280 ppm). Other researchers similarly found that

https://doi.org/10.5194/egusphere-2025-5436
Preprint. Discussion started: 18 November 2025

lowering atmospheric CO_2 concentrations to 280 ppm controlled the late Pliocene glaciation of Greenland in a fully coupled atmosphere–ocean general circulation model and an ice-sheet model (Lunt et al., 2008). Proxy data confirms that this carbon dioxide threshold likely was not crossed until the late Pliocene, ~2.7-2.8 Ma, and that decreasing levels of atmospheric CO_2 in the late Pliocene likely corresponded with cooling global temperatures (Bartoli et al., 2011; de la Vega et al., 2020; Stap et al., 2018).

Similarly, recent analyses of global temperature change during the past 4.5 million years by Clark et al. (2024) show that no region of the ocean displays an acceleration from the mean global cooling trend occurring throughout the Pliocene; this pattern is apparent even with the inclusion of what now turn out to be erroneously cold SST estimates from ODP 1090 (Martinez-Garcia et al., 2010).

Analyses using models from Phase 2 of the Pliocene Model Intercomparison Project (PlioMIP2) and paleoclimate proxy data from the PlioVAR working group conducted by Burton et al. (2024) indicate that at most sites, mid-Pliocene SST changes were forced by CO_2. Although they also utilize the SST record by Martínez-Garcia et al. (2010), they nevertheless found that changes in SST at ODP 1090 were found to be primarily driven by CO_2 forcings, and non-CO_2 forcings were dominant only at North Atlantic sites. However, the researchers also note that there is a significant, negative relationship between FCO_2 (the proportion of the total Pliocene minus preindustrial climate change that is due to CO_2 forcing; Burton et al., 2023) and data-model agreement at ODP 1090, with this agreement ranging from 0.35 °C (CESM2) to −2.98 °C (NorESM1-F) with a multi-model mean of −1.63 °C, indicating that the paleo-record suggested temperatures were on average colder than the model output (Burton et al., 2024). By utilizing our new, warmer SST estimates instead of the colder Martínez-Garcia record, data-model agreement at ODP Site 1090 would be improved: Over the time slice of analysis (MIS KM5c, 3.205 ± 0.01 Ma), our revised record of SST is on average 0.8°C warmer than Martínez-Garcia record, cutting the degree of disagreement in half.

Why might atmospheric CO_2 concentrations have fallen to levels that allowed brief Northern Hemisphere glaciations throughout the Pliocene, and later the extensive growth of Northern Hemisphere ice sheets? Changes in high-latitude oceanographic processes tied to the global carbon cycle may have driven both global temperature changes and glaciation (Herbert et al., 2010). Reconstructions of neodymium isotope ratios and carbonate ion saturation indicate that ocean circulation shifted in the late Pliocene, providing more water to the Pacific sourced from the Southern Ocean. They also suggest that respired carbon storage into the deep Pacific increased during the late Pliocene, possibly due to strengthened deep-water formation and biological-pump efficiency in the Southern Ocean due to the expansion of sea-ice (Jian et al., 2023). Continued proxy-studies regarding carbon sequestration, carbonate production, and the biologic pump in the late Pliocene may help to further explain how atmospheric CO_2 levels changed leading to iNHG.

6 Conclusions

https://doi.org/10.5194/egusphere-2025-5436
Preprint. Discussion started: 18 November 2025

We presented here a revised record of alkenone-derived sea surface temperatures (SSTs) from ODP Site 1090, a mid-latitude, open ocean site located in the subpolar southeast Atlantic Ocean. Rigorous extract cleanup and analytical methods, use of the $U^{k'}_{37}$ unsaturation index, and improved stratigraphy, produced a robust SST reconstruction from the late Pliocene. Our revised record suggests that sea surface temperatures at ODP Site 1090 were warmer than previously estimated, challenging the hypothesis that cooling and ice sheet expansion in the high-latitude Southern Hemisphere was the primary driver of iNHG. Our spectral analysis found that SST, like the global $\delta^{18}O_{benthic}$ stack, displayed similar amplification at the orbital scale in the late Pliocene. This agreement suggests that the same forcing may have controlled both the local SST and the controls on $\delta^{18}O_{benthic}$ (global ice volume and deepwater temperature), and it is consistent with the hypothesis that a global driver, such as deceasing atmospheric carbon dioxide concentrations, may have led to the intensification of Northern Hemisphere Glaciation (iNHG) in the late Pliocene.

Data Availability Statement

All utilized datasets are available via the PANGAEA online repository; they can be accessed through the citations given in Table 1, with full references provided below. All biomarker data presented in this study will be available in the PANGAEA database upon publishing (Felden et al., 2023).

Author Contributions

BH: methodology, GC-FID and HPLC-MS alkenone analyses, investigation, writing (original draft, review, and editing), data visualization. TDH: conceptualization, writing (review and editing), supervision, funding acquisition. JP: HPLC-MS methodology and alkenone analyses.

Competing Interests

The authors declare that they have no conflict of interest.

Acknowledgements

Thanks are owed to the IODP curators and staff for their work in maintaining the sediment archive and providing samples for this study, Xiangming Zhao and Naomi Hudis for conducting prior ODP 1090 analyses utilized in this study, and the crew and scientists of ODP Leg 177. Foundational work for this project was funded by NSF Grants OCE-1459280 & OCE-1545859.

References

Bard, E., & Rickaby, R. E. M. (2009). Migration of the subtropical front as a modulator of glacial climate. *Nature, 460*(7253), 380–383. https://doi.org/10.1038/nature08189

https://doi.org/10.5194/egusphere-2025-5436
Preprint. Discussion started: 18 November 2025

Bartoli, G., Hönisch, B., & Zeebe, R. E. (2011). Atmospheric CO2 decline during the Pliocene intensification of Northern Hemisphere glaciations. *Paleoceanography, 26*(4). https://doi.org/10.1029/2010PA002055

Becquey, S., & Gersonde, R. (2002). Past hydrographic and climatic changes in the Subantarctic Zone of the South Atlantic – The Pleistocene record from ODP Site 1090. *Palaeogeography, Palaeoclimatology, Palaeoecology, 182*(3), 221–239. https://doi.org/10.1016/S0031-0182(01)00497-7

Billups, K., Pälike, H., Channell, J. E. T., Zachos, J. C., & Shackleton, N. J. (2004). Astronomic calibration of the late Oligocene through early Miocene geomagnetic polarity time scale. *Earth and Planetary Science Letters*, *224*(1–2), 33–44. https://doi.org/10.1016/j.epsl.2004.05.004

Blake-Mizen, K., Hatfield, R. G., Stoner, J. S., Carlson, A. E., Xuan, C., Walczak, M., Lawrence, K. T., Channell, J. E. T., & Bailey, I. (2019). Southern Greenland glaciation and Western Boundary Undercurrent evolution recorded on Eirik Drift during the late Pliocene intensification of Northern Hemisphere glaciation. *Quaternary Science Reviews, 209*, 40–51. https://doi.org/10.1016/j.quascirev.2019.01.015

Brassell, S. C., Eglinton, G., Marlowe, I. T., Pflaumann, U., & Sarnthein, M. (1986). Molecular stratigraphy: A new tool for climatic assessment. *Nature, 320*(6058), 129–133. https://doi.org/10.1038/320129a0

Broccoli, A. J., & Manabe, S. (1987). The influence of continental ice, atmospheric CO2, and land albedo on the climate of the last glacial maximum. *Climate Dynamics, 1*(2), 87–99. https://doi.org/10.1007/BF01054478

Burke, K. D., Williams, J. W., Chandler, M. A., Haywood, A. M., Lunt, D. J., & Otto-Bliesner, B. L. (2018). Pliocene and Eocene provide best analogs for near-future climates. *Proceedings of the National Academy of Sciences, 115*(52), 13288–13293. https://doi.org/10.1073/pnas.1809600115

Burton, L. E., Haywood, A. M., Tindall, J. C., Dolan, A. M., Hill, D. J., McClymont, E. L., Ho, S. L., & Ford, H. L. (2024). The role of atmospheric CO2 in controlling sea surface temperature change during the Pliocene. *Climate of the Past, 20*(5), 1177–1194. https://doi.org/10.5194/cp-20-1177-2024

Clark, P. U., Shakun, J. D., Rosenthal, Y., Köhler, P., & Bartlein, P. J. (2024). Global and regional temperature change over the past 4.5 million years. *Science, 383*(6685), 884–890. https://doi.org/10.1126/science.adi1908

Conte, M. H., Sicre, M.-A., Rühlemann, C., Weber, J. C., Schulte, S., Schulz-Bull, D., & Blanz, T. (2006). Global temperature calibration of the alkenone unsaturation index (UK′37) in surface waters and comparison with surface sediments. *Geochemistry, Geophysics, Geosystems, 7*(2). https://doi.org/10.1029/2005GC001054

D'Andrea, W. J., & Huang, Y. (2005). Long chain alkenones in Greenland lake sediments: Low δ 13C values and exceptional abundance. *Organic Geochemistry, 36*(9), 1234–1241. https://doi.org/10.1016/j.orggeochem.2005.05.001

D'Andrea, W. J., Liu, Z., Alexandre, M. D. R., Wattley, S., Herbert, T. D., & Huang, Y. (2007). An Efficient Method for Isolating Individual Long-Chain Alkenones for Compound-Specific Hydrogen Isotope Analysis. *Analytical Chemistry, 79*(9), 3430–3435. https://doi.org/10.1021/ac062067w

de la Vega, E., Chalk, T. B., Wilson, P. A., Bysani, R. P., & Foster, G. L. (2020). Atmospheric CO2 during the Mid-Piacenzian Warm Period and the M2 glaciation. *Scientific Reports, 10*(1), 11002. https://doi.org/10.1038/s41598-020-67154-8

https://doi.org/10.5194/egusphere-2025-5436
Preprint. Discussion started: 18 November 2025

DeConto, R. M., Pollard, D., Wilson, P. A., Pälike, H., Lear, C. H., & Pagani, M. (2008). Thresholds for Cenozoic bipolar glaciation. *Nature, 455*(7213), 652–656. https://doi.org/10.1038/nature07337

Dillon, J. (2023). Chemplexity/chromatography-gui [Matlab]. https://github.com/chemplexity/chromatography-gui (Original work published 2017)

Etourneau, J., Schneider, R., Blanz, T., & Martinez, P. (2010a). Intensification of the Walker and Hadley atmospheric circulations during the Pliocene–Pleistocene climate transition. *Earth and Planetary Science Letters, 297*(1), 103–110. https://doi.org/10.1016/j.epsl.2010.06.010

Etourneau, J., Schneider, R. R., Blanz, T., & Martinez, P. (2010b). (Appendix 3) UK'37 index and sea surface temperature reconstruction of ODP Hole 177-1090D [dataset]. In supplement to: Etourneau, J et al. (2010): Intensification of the Walker and Hadley atmospheric circulations during the Pliocene-Pleistocene climate transition. *Earth and Planetary Science Letters, 297*(1-2), 103-110, https://doi.org/10.1016/j.epsl.2010.06.010. PANGAEA. https://doi.org/10.1594/PANGAEA.786700

Felden, J., Möller, L., Schindler, U., Huber, R., Schumacher, S., Koppe, R., Diepenbroek, M., & Glöckner, F. O. (2023). *PANGAEA - Data Publisher for Earth & Environmental Science. Scientific Data, 10*(1), 347. https://doi.org/10.1038/s41597-023-02269-x

Flesche Kleiven, H., Jansen, E., Fronval, T., & Smith, T. M. (2002). Intensification of Northern Hemisphere glaciations in the circum Atlantic region (3.5–2.4 Ma) – ice-rafted detritus evidence. *Palaeogeography, Palaeoclimatology, Palaeoecology, 184*(3), 213–223. https://doi.org/10.1016/S0031-0182(01)00407-2

Haug, G. H., & Tiedemann, R. (1998). Effect of the formation of the Isthmus of Panama on Atlantic Ocean thermohaline circulation. *Nature, 393*(6686), 673–676. https://doi.org/10.1038/31447

Haywood, A. M., Hill, D. J., Dolan, A. M., Otto-Bliesner, B. L., Bragg, F., Chan, W.-L., Chandler, M. A., Contoux, C., Dowsett, H. J., Jost, A., Kamae, Y., Lohmann, G., Lunt, D. J., Abe-Ouchi, A., Pickering, S. J., Ramstein, G., Rosenbloom, N. A., Salzmann, U., Sohl, L., … Zhang, Z. (2013). Large-scale features of Pliocene climate: Results from the Pliocene Model Intercomparison Project. *Climate of the Past, 9*(1), 191–209. https://doi.org/10.5194/cp-9-191-2013

Herbert, T. D. (2003). 6.15—Alkenone Paleotemperature Determinations. In H. D. Holland & K. K. Turekian (Eds.), *Treatise on Geochemistry* (pp. 391–432). Pergamon. https://doi.org/10.1016/B0-08-043751-6/06115-6

Herbert, Timothy D; Caballero-Gill, Rocio P; Novak, Joseph B (2020): Revised sea surface temperature (SST) and alkenone data for the late Pliocene composite section from different Holes of ODP Site 138-846 [dataset]. PANGAEA, https://doi.org/10.1594/PANGAEA.912758, In: Herbert, TD et al. (2021): Revised late Pliocene composite section for ODP Site 138-846 [dataset bundled publication]. PANGAEA, https://doi.org/10.1594/PANGAEA.931478

Herbert, T. D., Peterson, L. C., Lawrence, K. T., & Liu, Z. (2010). Tropical Ocean Temperatures Over the Past 3.5 Million Years. *Science, 328*(5985), 1530–1534. https://doi.org/10.1126/science.1185435

Jansen, E., Fronval, T., Rack, F., & Channell, J. E. T. (2000). Pliocene-pleistocene ice rafting history and cyclicity in the Nordic seas during the last 3.5 myr. *Paleoceanography, 15*(6), 709–721. Scopus. https://doi.org/10.1029/1999PA000435

https://doi.org/10.5194/egusphere-2025-5436
Preprint. Discussion started: 18 November 2025

Jian, Z., Dang, H., Yu, J., Wu, Q., Gong, X., Stepanek, C., Colin, C., Hu, L., Lohmann, G., Zhou, X., & Wan, S. (2023). Changes in deep Pacific circulation and carbon storage during the Pliocene-Pleistocene transition. *Earth and Planetary Science Letters, 605*, 118020. https://doi.org/10.1016/j.epsl.2023.118020

Kimble, Kristin; Herbert, Timothy D; Jones, Colin (2024): Sea surface temperature from ODP Site 138-846 [dataset]. PANGAEA, https://doi.org/10.1594/PANGAEA.962707, In: Kimble, K., et al. (2024): Pliocene alkenone sea surface temperature and productivity gradients at eastern equatorial Pacific ODP Sites 138-846, 849 and IODP Site 321-U1338 [dataset bundled publication]. PANGAEA, https://doi.org/10.1594/PANGAEA.962716

Laskar, J., Fienga, A., Gastineau, M., & Manche, H. (2011). La2010: A new orbital solution for the long-term motion of the Earth. *Astronomy & Astrophysics, 532*, A89. https://doi.org/10.1051/0004-6361/201116836

Lawrence, K.T.; Liu, Z.; Herbert, T.D. (2006-07-01): NOAA/WDS Paleoclimatology - Lawrence et al. 2006 Eastern Equatorial Pacific 5MMYr Alkenone SST Reconstruction. NOAA National Centers for Environmental Information. https://doi.org/10.25921/tc81-tf95.

Lear, C. H., Bailey, T. R., Pearson, P. N., Coxall, H. K., & Rosenthal, Y. (2008). Cooling and ice growth across the Eocene-Oligocene transition. *Geology, 36*(3), 251–254. https://doi.org/10.1130/G24584A.1

Liao, S., Liu, X.-L., Manz, K. E., Pennell, K. D., Novak, J., Santos, E., & Huang, Y. (2023). Comprehensive analysis of alkenones by reversed-phase HPLC-MS with unprecedented selectivity, linearity and sensitivity. *Talanta, 260*, 124653. https://doi.org/10.1016/j.talanta.2023.124653

Liao, S., Wang, K. J., & Huang, Y. (2023). Unusually high production of C37:4 alkenone by an Arctic Gephyrocapsa huxleyi strain grown under nutrient-replete conditions. *Organic Geochemistry, 177*, 104539. https://doi.org/10.1016/j.orggeochem.2022.104539

Lisiecki, L. E., & Raymo, M. E. (2005). A Pliocene-Pleistocene stack of 57 globally distributed benthic δ18O records. *Paleoceanography, 20*(1). https://doi.org/10.1029/2004PA001071

Lunt, D. J., Foster, G. L., Haywood, A. M., & Stone, E. J. (2008). Late Pliocene Greenland glaciation controlled by a decline in atmospheric CO2 levels. *Nature, 454*(7208), 1102–1105. https://doi.org/10.1038/nature07223

Lunt, D. J., Valdes, P. J., Haywood, A., & Rutt, I. C. (2008). Closure of the Panama Seaway during the Pliocene: Implications for climate and Northern Hemisphere glaciation: Climate Dynamics. *Climate Dynamics, 30*(1), 1–18. https://doi.org/10.1007/s00382-007-0265-6

Marlowe, I. T., Green, J. C., Neal, A. C., Brassell, S. C., Eglinton, G., & Course, P. A. (1984). Long chain (n-C37–C39) alkenones in the Prymnesiophyceae. Distribution of alkenones and other lipids and their taxonomic significance. *British Phycological Journal, 19*(3), 203–216. https://doi.org/10.1080/00071618400650221

Martin, C., Richter, N., Lloren, R., & Dubois, N. (2024). Impact of saponification and silver-nitrate purification on lacustrine alkenone distributions and alkenone-based indices. *Journal of Chromatography A, 1715*, 464576. https://doi.org/10.1016/j.chroma.2023.464576

https://doi.org/10.5194/egusphere-2025-5436
Preprint. Discussion started: 18 November 2025

Martínez-Garcia, A., Rosell-Melé, A., Geibert, W., Gersonde, R., Masqué, P., Gaspari, V., & Barbante, C. (2009). Links between iron supply, marine productivity, sea surface temperature, and CO2 over the last 1.1 Ma. *Paleoceanography, 24*(1). https://doi.org/10.1029/2008PA001657

Martínez-Garcia, A., Rosell-Melé, A., Jaccard, S. L., Geibert, W., Sigman, D. M., & Haug, G. H. (2011). Southern Ocean dust–climate coupling over the past four million years. *Nature, 476*(7360), 312–315. https://doi.org/10.1038/nature10310

Martínez-Garcia, A., Rosell-Melé, A., McClymont, E. L., Gersonde, R., & Haug, G. H. (2010). Subpolar Link to the Emergence of the Modern Equatorial Pacific Cold Tongue. *Science, 328*(5985), 1550–1553. https://doi.org/10.1126/science.1184480

Martínez-García, A., Rosell-Melé, A., McClymont, E. L., Gersonde, R., & Haug, G. H. (2010). (Table S2) Sea surface temperature and relative abundance of $C_{37:4}$ alkenone in ODP Site 177-1090 [dataset]. In In supplement to: Martínez-García, A et al. (2010): Subpolar Link to the Emergence of the Modern Equatorial Pacific Cold Tongue. *Science, 328*(5985), 1550-1553, https://doi.org/10.1126/Science.1184480. PANGAEA. https://doi.org/10.1594/PANGAEA.771706

McClymont, E. L., Ho, S. L., Ford, H. L., Bailey, I., Berke, M. A., Bolton, C. T., De Schepper, S., Grant, G. R., Groeneveld, J., Inglis, G. N., Karas, C., Patterson, M. O., Swann, G. E. A., Thirumalai, K., White, S. M., Alonso-Garcia, M., Anand, P., Hoogakker, B. a. A., Littler, K., … Tangunan, D. (2023). Climate Evolution Through the Onset and Intensification of Northern Hemisphere Glaciation. *Reviews of Geophysics, 61*(3), e2022RG000793. https://doi.org/10.1029/2022RG000793

McKay, R., Naish, T., Carter, L., Riesselman, C., Dunbar, R., Sjunneskog, C., Winter, D., Sangiorgi, F., Warren, C., Pagani, M., Schouten, S., Willmott, V., Levy, R., DeConto, R., & Powell, R. D. (2012). Antarctic and Southern Ocean influences on Late Pliocene global cooling. *Proceedings of the National Academy of Sciences, 109*(17), 6423–6428. https://doi.org/10.1073/pnas.1112248109

Meyers, S., Malinverno, A., Hinnov, L., Zeeden, C., Liu, H., & Moron, V. (2021). Astrochron: A computational tool for astrochronology (Vol. 144).

Müller, P. J., Kirst, G., Ruhland, G., von Storch, I., & Rosell-Melé, A. (1998). Calibration of the alkenone paleotemperature index U37K′ based on core-tops from the eastern South Atlantic and the global ocean (60°N-60°S). *Geochimica et Cosmochimica Acta, 62*(10), 1757–1772. https://doi.org/10.1016/S0016-7037(98)00097-0

NOAA Global Monitoring Laboratory. (2025). Trends in CO2, CH4, N2O, SF6: Trends in Atmospheric Carbon Dioxide (CO2). https://gml.noaa.gov/ccgg/trends/

Novak, J., McGrath, S. M., Wang, K. J., Liao, S., Clemens, S. C., Kuhnt, W., & Huang, Y. (2022). UK'38 Expands the linear dynamic range of the alkenone sea surface temperature proxy. *Geochimica et Cosmochimica Acta, 328*, 207–220. https://doi.org/10.1016/j.gca.2022.04.021

Prahl, F. G., Muehlhausen, L. A., & Zahnle, D. L. (1988). Further evaluation of long-chain alkenones as indicators of paleoceanographic conditions. *Geochimica et Cosmochimica Acta, 52*(9), 2303–2310. https://doi.org/10.1016/0016-7037(88)90132-9

https://doi.org/10.5194/egusphere-2025-5436
Preprint. Discussion started: 18 November 2025

Prahl, F. G., & Wakeham, S. G. (1987). Calibration of unsaturation patterns in long-chain ketone compositions for palaeotemperature assessment. *Nature, 330*(6146), 367–369. https://doi.org/10.1038/330367a0

Raberg, J. H., Harning, D. J., Crump, S. E., De Wet, G., Blumm, A., Kopf, S., Geirsdóttir, Á., Miller, G. H., & Sepúlveda, J. (2021). Revised fractional abundances and warm-season temperatures substantially improve brGDGT calibrations in lake sediments. *Biogeosciences, 18*(12), 3579–3603. https://doi.org/10.5194/bg-18-3579-2021

Rae, J. W. B., Zhang, Y. G., Liu, X., Foster, G. L., Stoll, H. M., & Whiteford, R. D. M. (2021). Atmospheric CO2 over the Past 66 Million Years from Marine Archives. *Annual Review of Earth and Planetary Sciences, 49*(Volume 49, 2021), 609–641. https://doi.org/10.1146/annurev-earth-082420-063026

Reid, J. L. (1989). On the total geostrophic circulation of the South Atlantic Ocean: Flow patterns, tracers, and transports. *Progress in Oceanography, 23*(3), 149–244. https://doi.org/10.1016/0079-6611(89)90001-3

Shipboard Scientific Party. (1999). Proceedings of the Ocean Drilling Program, Initial Reports (177; pp. 1–66). Ocean Discovery Program (ODP). doi:10.2973/odp.proc.ir.177.1999

Sikes, E. L., Farrington, J. W., & Keigwin, L. D. (1991). Use of the alkenone unsaturation ratio U37k to determine past sea surface temperatures: Core-top SST calibrations and methodology considerations. *Earth and Planetary Science Letters, 104*(1), 36–47. https://doi.org/10.1016/0012-821X(91)90235-A

Stap, L. B., van de Wal, R. S. W., de Boer, B., Köhler, P., Hoencamp, J. H., Lohmann, G., Tuenter, E., & Lourens, L. J. (2018). Modeled Influence of Land Ice and CO2 on Polar Amplification and Paleoclimate Sensitivity During the Past 5 Million Years. *Paleoceanography and Paleoclimatology, 33*(4), 381–394. https://doi.org/10.1002/2017PA003313

Tan, Ning, Ramstein, Gilles, Dumas, Christophe, Contoux, Camille, Ladant, Jean-Baptiste, Sepulchre, Pierre, Zhang, Zhongshi, & De Schepper, Stijn. (2017). Exploring the MIS M2 glaciation occurring during a warm and high atmospheric CO2 Pliocene background climate. *Earth and Planetary Science Letters*, *472*, 266–276. https://doi.org/10.1016/j.epsl.2017.04.050

Thiede, J., Jessen, C., Knutz, P., Kuijpers, A., Mikkelsen, N., Nørgaard-Pedersen, N., & Spielhagen, R. F. (2011). Millions of Years of Greenland Ice Sheet History Recorded in Ocean Sediments. *Polarforschung; Alfred Wegener Institute for Polar and Marine Research & German Society of Polar Research*. https://epic.awi.de/id/eprint/30005/

Tierney, J. E., & Tingley, M. P. (2018). BAYSPLINE: A New Calibration for the Alkenone Paleothermometer. *Paleoceanography and Paleoclimatology, 33*(3), 281–301. https://doi.org/10.1002/2017PA003201

Wang, K. J., Huang, Y., Majaneva, M., Belt, S. T., Liao, S., Novak, J., Kartzinel, T. R., Herbert, T. D., Richter, N., & Cabedo-Sanz, P. (2021). Group 2i Isochrysidales produce characteristic alkenones reflecting sea ice distribution. *Nature Communications, 12*(1), 15. https://doi.org/10.1038/s41467-020-20187-z

Willeit, M., Ganopolski, A., Calov, R., Robinson, A., & Maslin, M. (2015). The role of CO2 decline for the onset of Northern Hemisphere glaciation. *Quaternary Science Reviews, 119,* 22–34. https://doi.org/10.1016/j.quascirev.2015.04.015

Woodard, S. C., Rosenthal, Y., Miller, K. G., Wright, J. D., Chiu, B. K., & Lawrence, K. T. (2014). Antarctic role in Northern Hemisphere glaciation. *Science, 346*(6211), 847–851. https://doi.org/10.1126/science.1255586

https://doi.org/10.5194/egusphere-2025-5436
Preprint. Discussion started: 18 November 2025

Zachos, J., Pagani, M., Sloan, L., Thomas, E., & Billups, K. (2001). Trends, Rhythms, and Aberrations in Global Climate 65 Ma to Present. *Science, 292*(5517), 686–693. https://doi.org/10.1126/science.1059412